THE JOURNAL OF BIOLOGICAL CHEMISTRY
Vol. 279, No. 19, Issue of May 7, pp. 20009–20017, 2004

Printed in U.S.A.

The Hydrophobic Recognition Site Formed by Residues PsaA-Trp^{651} and PsaB-Trp^{627} of Photosystem I in *Chlamydomonas reinhardtii* Confers Distinct Selectivity for Binding of Plastocyanin and Cytochrome c_6*

Received for publication, December 22, 2003, and in revised form, February 25, 2004
Published, JBC Papers in Press, March 2, 2004, DOI 10.1074/jbc.M313986200

Frederik Sommer‡, Friedel Drepper¶, Wolfgang Haehnel¶, and Michael Hippler‡§

From the ‡Lehrstuhl für Pflanzenphysiologie, Friedrich-Schiller-Universität Jena, Dornburgerstr. 159, 07743 Jena, Germany and the ¶Biochemie der Pflanzen, Universität Freiburg, Schänzlestr. 1, 79104 Freiburg, Germany

On the lumenal side of photosystem I (PSI), each of the two large core subunits, PsaA and PsaB, expose a conserved tryptophan residue to the surface. PsaB-Trp^{627} is part of the hydrophobic recognition site that is essential for tight binding of the two electron donors plastocyanin and cytochrome c_6 to the donor side of PSI (Sommer, F., Drepper, F., and Hippler, M. (2002) *J. Biol. Chem.* 277, 6573–6581). To examine the function of PsaA-Trp^{651} in binding and electron transfer of both donors to PSI, we generated the mutants PsaA-W651F and PsaA-W651S by site-directed mutagenesis and biolistic transformation of *Chlamydomonas reinhardtii*. The protein-protein interaction and the electron transfer between the donors and PSI isolated from the mutants were analyzed by flash absorption spectroscopy. The mutation PsaA-W651F completely abolished the formation of a first order electron transfer complex between plastocyanin (pc) and the altered PSI and increased the dissociation constant for binding of cytochrome (cyt) c_6 by more than a factor of 10 as compared with wild type. Mutation of PsaA-Trp^{651} to Ser had an even larger impact on the dissociation constant. The K_D value increased another 2-fold when the values obtained for the interaction and electron transfer between cyt c_6 and PSI from PsaA-W651S and PsaA-W651F are compared. In contrast, binding and electron transfer of pc to PSI from PsaA-W651S improved as compared with PSI from PsaA-W651F and admitted the formation of an intermolecular electron transfer complex, resulting in a K_D value of about 554 μM that is still five times higher than observed for wild type. These results demonstrate that PsaA-Trp^{651} is, such as PsaB-Trp^{627}, crucial for high affinity binding of pc and cyt c_6 to PSI. Our results also indicate that the highly conserved structural recognition motif that is formed by PsaA-Trp^{651} and PsaB-Trp^{627} confers a differential selectivity in binding of both donors to PSI.

Photosystem I (PSI)[1] is an integral light-driven plastocyanin:ferredoxin oxidoreductase that is embedded in the thylakoid membrane. It is a multiprotein complex that uses light energy to transport electrons from the lumenal soluble electron carrier plastocyanin (pc) across the membrane to the stromal soluble electron acceptor ferredoxin. In cyanobacteria and green algae, cytochrome c_6 (cyt c_6) can substitute pc depending on the availability of copper in the medium (1–4). The crystal structure of PSI from *Synechococcus elongatus* has been refined to a resolution of 2.5 Å (5). PSI of *Chlamydomonas reinhardtii* consists of about 14 subunits (6), of which PsaA and PsaB form the core of the complex, each carrying a set of cofactors required for a functional electron transport chain through PSI. The 4Fe-4S cluster F_X is located on both PsaA and PsaB, and the terminal 4Fe-4S clusters F_A and F_B are bound to PsaC on the stromal side where binding of ferredoxin takes place facilitated by PsaC, PsaD, and PsaE (7).

On the lumenal side of PSI, the primary electron donor P700, a chlorophyll *a* dimer, is located near the lumenal surface. It is separated from the lumenal space by two α helices, l' and l, formed by loops j' and j in PsaA and PsaB, respectively, which are arranged in parallel to the membrane plane. A characteristic feature for PsaF from algae and vascular plants is an extension of its lumenal N-terminal domain that is absent from cyanobacteria and that was proposed to form an amphipatic helix with basic patches facing the binding site of the soluble electron donors (8). The electron transfer to eukaryotic PSI shows a multifaceted kinetic behavior and can be described by a multistep process involving donor binding, PSI-donor complex formation, electron transfer, and unbinding of the donor (9). Docking of pc or cyt c_6 to the PSI is mainly promoted by two highly conserved structural interaction patterns, which are (i) long range electrostatic attractions between basic patches of PsaF and acidic regions of pc and cyt c_6 (8, 10–13) and (ii) a hydrophobic region around the electron transfer site of the donors interacting with a hydrophobic region site on PSI including PsaB-Trp^{627} in *C. reinhardtii* (11, 14).

The function of the positively charged residues in the eukaryotic N terminus of PsaF in binding of both donors has been studied extensively by cross-linking, knock-out, and reverse genetics experiments (8, 13, 15–17). These studies showed that the basic patch present in the N-terminal domain of PsaF is crucial for proper binding, complex formation between donor and PSI, and fast electron transfer. It is of note that the existence and the discussed function of the eukaryotic N-terminal domain of PsaF is supported by the new crystal structure data on plant PSI (18). In contrast to eukaryotic organisms in the cyanobacterium *Synechocystis* sp. PCC 6803, efficient binding and electron transfer between PSI and pc or cyt c_6 does not depend on the PsaF subunit since the specific deletion of the *psaF* gene in cyanobacteria did not affect photoautotrophic

* This work has been supported by a grant of the Federal State of Thüringen (Nachwuchsgruppe Pflanzenphysiologie) (to M. H.). The costs of publication of this article were defrayed in part by the payment of page charges. This article must therefore be hereby marked "*advertisement*" in accordance with 18 U.S.C. Section 1734 solely to indicate this fact.

§ To whom correspondence should be addressed: Dept. of Biology, University of Pennsylvania, Philadelphia, PA 19104. Tel.: 215-898-4974; 215-898-8780; E-mail: mhippler@sas.upenn.edu.

[1] The abbreviations used are: PSI, photosystem I; WT, wild type; pc, plastocyanin; cyt, cytochrome.

growth (19) and the *in vivo* and *in vitro* measured electron transfer rate between cyt c_{553} and PSI was the same as in WT (20).

The hydrophobic interaction site of the PSI core formed by PsaB has been studied by site-directed mutagenesis. Sun *et al.* (21) introduced short stretches of mutations in the lumenal loop *j* of the PsaB protein from *Synechocystis* sp. PCC 6803 and could isolate a double mutant (W622C/A623R), which was highly photosensitive and showed a severe defect in the interaction with pc or cyt c_6. A more conservative mutation of Trp^{627} (corresponding to Trp^{622} in *Synechocystis* and Trp^{631} in *S. elongatus*) to Phe in the eukaryotic PSI of *C. reinhardtii* also displayed a strong effect on growth (14). Cells became strongly photosensitive, and *in vitro* analysis of the electron transfer reactions revealed a differential effect on the binding constants of pc and cyt c_6. No complex formation was observed for the interaction of pc with the altered PSI, whereas it was still present with cyt c_6, displaying a 10-fold decreased electron transfer rate. Interestingly, as seen from the crystal structure, Trp^{631} in loop *j* of PsaB (corresponding to Trp^{627} in *C. reinhardtii*) forms a sandwich complex with the corresponding Trp^{655} of PsaA (corresponding to Trp^{651} in *C. reinhardtii*). This stacked π-electron system is located in close distance to P700.

In this study, we questioned the role of PsaA-Trp^{651} for binding and electron transfer between PSI and pc or cyt c_6. Mutants PsaA-W651F and PsaA-W651S were generated by site-directed mutagenesis and biolistic transformation of *C. reinhardtii*. Both mutations had large effects on the *in vitro* measured electron transfer kinetics between pc or cyt c_6 and the altered PSI. The results are discussed in respect to the function of residue PsaB-W627F in binding and electron transfer between the donors and PSI.

MATERIALS AND METHODS

Strains and Media—*C. reinhardtii* wild-type and mutant strains were grown as described (22). If necessary, the media (Tris acetate phosphate medium or high salt minimal medium) were solidified with 1.5% Kolbe agar (Roth) and supplemented with 150 μg/ml spectinomycin (Sigma) when required.

Nucleic Acid Techniques—*In vitro* site-directed mutagenesis was performed according to standard protocols (23) using *Escherichia coli* strain DH5α as a bacterial host. For the single exchange of PsaA-Trp^{651}, PCR was performed using as template plasmid pKR154 (24) containing the *psaA* gene and the *aadA*-cassette (25) and using as mutation-carrying primers 5′-GGTTACGTGACTTCTTATTTGCACAATCATCA-C-3′ and the antisense oligonucleotide for the exchange of PsaA-Trp^{651} to Phe or 5′-CGTGACTTCTTATCGGCACAATC-3′ and the antisense oligonucleotide for the exchange PsaA-W651S. After PCR, the template was DpnI-digested, and the PCR product was transformed and amplified in *E. coli*. The mutations were verified by sequencing. Biolistic transformation of chloroplasts using the PDS-1000/He device (Bio-Rad) and selection on spectinomycin was carried out as described (14). As the recipient strain, ΔPsaA cells lacking the *psaA* gene were chosen (24).

Isolation of Proteins from C. reinhardtii—Thylakoid membranes and PSI from wild-type and mutant strains were isolated as described (12), and chlorophyll content was determined according to Porra *et al.* (26). Isolation of pc and cyt c_6 was done as published (12), and the concentrations of pc and cyt c_6 were determined spectroscopically using an extinction coefficient of 4.9 mM^{-1} cm^{-1} at 597 nm for the oxidized form of pc and 20 mM^{-1} cm^{-1} at 552 nm for the reduced form of cyt c_6.

SDS-PAGE and Immuno-analysis—SDS-PAGE (15.5% T, 2.66% C), was carried out as described (27). Western blotting and immuno-detection followed the protocols according to Hippler *et al.* (12). For the quantification of PSI content in mutant strains as compared with wild type, different amounts of the thylakoid fraction isolated from wild type supplemented with thylakoids from the PSI lacking the ΔPsaB strain to a final amount of 20 μg of proteins were fractionated on a SDS-PAGE gel together with thylakoids isolated from mutant strains according to 20 μg of proteins. Immuno-analysis was carried out using anti-PsaF antibodies and anti-LHCII (light-harvesting proteins of PSII) antibodies to verify equal loading.

Cross-linking Procedure—Cross-linking was performed as described (12).

Redox Potentiometry—Determination of the redox midpoint potential for P700/$P700^+$ from WT and the different mutant strains was done essentially as described (9). A cuvette with an optical path length of 10 mm containing 3.5 ml of sample under argon was used. As redox mediators, duroquinone and *N*,*N*,*N*′,*N*′-tetramethyl-p-phenylenediamine at 5 μM, ferro- and ferricyanide at 10 μM, and pc at 2 μM were added, and the redox potential was adjusted by additions of ferricyanide or ascorbate. For measurement of the redox potential, a platinum electrode and an Ag/AgCl reference electrode were used. Calibration of the reference electrode was done with quinhydrone at a given pH and a ferro-/ferricyanide system displaying an error of ±5 mV (n = 4). Midpoint redox potentials were determined by fitting the redox titration data to Nernst equation curves using a non-linear curve-fitting program (ORIGIN v4.10, Microcal Software). All redox potentials are displayed relative to the standard hydrogen electrode.

Flash Absorption Spectroscopy—Kinetics of flash-induced absorbance changes at 817 nm were measured essentially as described (9). The cuvette contained 200 μl of the sample and had an optical path length of 1 cm for the measuring light and of ~3 mm for the actinic light.

Analysis of the electron transfer kinetics was performed essentially as described (9, 13). Kinetic curves were deconvoluted where necessary into three distinct kinetic components by using a least square fit based on a Marquardt algorithm. The two faster kinetic components, with half-lives of $t_{1/2}$ in the range of μs to a few ms, which were mainly affected by the concentration of the donor, were used for further analysis of the binding and electron transfer of the donor to PSI. The analysis was based on the model described in Ref. 9 assuming a simple dissociation equilibrium for the complex between the reduced donor protein and PSI. The relative amplitude of the fast (μs) kinetic phase of the $P700^+$ reduction kinetics is described by

$$\mathrm{relA}(1) = f \times \frac{[D]}{[D] \times K_D} \qquad \text{(Eq. 1)}$$

where $[D]$ gives the concentration of the reduced donor, K_D gives the dissociation constant, and f represents an empirical factor ($f < 1$) that relates to the amplitude A(1) observed after the flash to the fraction of PSI in a complex with the reduced donor prior to the flash (9). The second kinetic phase, which is assumed to originate from a bimolecular reaction between PSI and the soluble donor, was analyzed as a pseudo first order reaction because in all experiments, the donor concentration exceeded the concentration of PSI by more than 1 order of magnitude. The second order rate constant k_2 was determined from experiments at donor concentrations where the reaction rate ($\ln 2/t_{1/2}(2)$) of the exponential time course increased linearly with increasing concentration by using the relation $k_2 = \ln 2/(t_{1/2}(2) \cdot [D])$.

A global fit analysis was used to improve the determination of the amplitude A(1) because its relative amplitude was very low (< ~0.2) at low donor concentrations in experiments with the mutated PSI. A sum of three exponentials was fitted simultaneously to six individual kinetic traces measured at different donor concentrations using the same value of the half-time of the fast kinetic phase $t_{1/2}(1)$ for each kinetic trace. The global curve-fitting was also used for the evaluation of kinetic traces measured in the presence of high concentrations of $MgCl_2$ (>30 mM) since the slowest and the intermediate kinetic phase had half-times in the same (ms) time range under these conditions. In this case, a constant ratio of the amplitudes was assumed that was derived from measurements at concentrations below 30 mM $MgCl_2$. All fits were performed on two independent sets of measurements.

RESULTS

Growth Properties—To investigate the impact of PsaA-Trp^{651} on the binding and the electron transport from pc or cyt c_6 to PSI, we performed site-specific mutagenesis and altered this residue to Phe and Ser. A plasmid containing the altered PsaA together with the aadA cassette conferring resistance to spectomycin was introduced into the *C. reinhardtii* strain ΔPsaA, lacking *psaA*, by biolistic transformation. The growth properties of the resulting mutant strains PsaA-W651F and PsaA-W651S were investigated. Hereby the mutant strains together with a WT strain were spotted on plates containing different media (Tris acetate phosphate and high salt minimal media) that were exposed to different light intensities and atmospheric conditions (Table I). All strains were able to grow

TABLE I

Growth inhibition of mutants under high light is restored under anaerobic conditions

Cells from liquid cultures were spotted on plates containing Tris acetate phosphate or high salt minimal medium for heterotrophic or photoautotrophic growth respectively and placed under different atmospheric and light conditions.

Strain	AEROB				ANAEROB	
	TAP	HSM	TAP	HSM	TAP	HSM
	60 μE/m²s[a]	*60 μE/m²s*	*700 μE/m²s*	*700 μE/m²s*	*700 μE/m²s*	*700 μE/m²s*
WT	++	++	++	++	++	++
PsaA-W651F	++	++	+	−	++	++
PsaA-W651S	++	++	+	−	++	++

[a] E, einstein.

heterotrophically under normal atmospheric conditions and all light intensities were tested, whereas under photoautotrophic conditions, the mutant strains became sensitive to light intensities higher than 700 microeinsteins m^{-2} s^{-1}. Photoautotrophic growth could be restored under anaerobic conditions, indicating that the production of reactive oxygen species under aerobic conditions could be a cause for the photosensitivity of both mutant strains. This is in line with observations made for other mutants affected at either the donor side or the acceptor side of PSI, where additionally increased lipid peroxidation as a consequence of high light treatment under aerobic conditions was reported (28).

PSI Content—To test whether the mutations affected the amount of PSI present in the mutant strains, thylakoids were isolated from both mutants and fractionated by SDS-PAGE. PSI was detected by Western blotting using PsaF-specific antibodies (Fig. 1), and the amount was estimated by comparison with the PsaF signal originated from a dilution series of wild-type thylakoids. The PSI content in strain PsaA-W651S or strain PsaA-W651F could be estimated to be above 70% as compared with WT. Therefore, the light sensitivity of both strains cannot be explained by a decrease in PSI content.

Cross-linking Experiments of Wild-type and Mutant PSI with pc or cyt c_6—To assess the binding and accessibility of PsaF for the two electron donors in wild type and the mutant PSI complexes, we performed cross-linking experiments using the zero-length linker EDC/NHS that leads to the formation of covalent bonds between the basic and acidic patches of PsaF and pc or cyt c_6, respectively. After cross-linking, the reaction mixture was fractionated by SDS-PAGE and analyzed by Western blotting using anti-PsaF antibodies. The heme group of cyt c_6 gives an antibody-independent light reaction in the presence of ECL and is also detectable in Fig. 2. PsaF could be cross-linked to both donors in wild-type and mutant PsaA-W651F. Although the cross-linking product between PSI from PsaA-W651S and cyt c_6 could only be detected as a weak band, it was clearly detectable between pc and PsaF from mutant PsaA-W651S. Thus, the interaction between PsaF of PSI PsaA-W651S and cyt c_6 appears to be strongly disturbed.

Incubation of the different PSI particles with the cross-linking mixture in the absence of donor gave rise to an additional band detectable with the anti-PsaF antibodies and migrating about 2–5 kDa above the PsaF band. In the presence of the electron donors, this band disappeared completely for wild-type PSI but was still detectable to some extent for the altered PSI complexes (Fig. 2).

Flash Absorption Spectroscopy—The effects of the mutations on binding and electron transfer between the two donors pc or cyt c_6 and PSI was analyzed by using flash-induced time-resolved absorption spectroscopy. We measured the kinetics of the absorption changes at 817 nm caused by P700 oxidation induced by a single flash and the subsequent reduction of $P700^+$ by soluble donors. Fig. 3 shows absorption transients for the altered PSI in the presence of 200 μM pc (*left panel*) or 300 μM cyt c_6 (*right panel*), respectively. In both mutants, the kinetics are drastically slowed down as compared to those with WT PSI (not shown, see Ref. 12). In WT PSI, the reduction of $P700^+$ by either of the two electron donors consisted of three distinct kinetic components: a fast first order phase with a half-time of $t_{½}(1)$ of 3–4 μs being independent of the concentration of pc or cyt c_6 and an amplitude A(1) that increased with increasing concentration of the donors, a slower second order component the half-life $t_{½}(2)$ (μs to ms range) and amplitude A(2) that depended on the donor concentration, and a third component (100 ms to s time range) that is assumed to derive from very slow ascorbate reduction of pc and/or damaged PSI that is only accessible for the donors at very slow rates. Therefore, for further discussion, we will only consider the two former components.

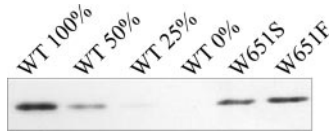

FIG. 1. **PSI content in mutants PsaA-W651F/S is only slightly reduced.** Thylakoids (20 μg of proteins) isolated from WT and mutants PsaA-W651F and PsaA-W651S as well as from a PSI-deficient mutant (ΔPsaB) were separated by SDS-PAGE and immuno-blotted. The blots were probed with anti-PsaF antibodies. To estimate the relative amount of PSI, thylakoids from WT were diluted with thylakoids from ΔPsaB (PSI-lacking) by keeping the total protein concentration constant.

Reduction of PSI PsaA-W651F by pc follows a monoexponential time course in the time range shown (Fig. 3*A*). A fast (μs) phase as found for wild-type PSI in the presence of 200 μM pc is not detectable, which indicates that binding between the reduced PSI and pc prior to flash oxidation is strongly disturbed. In contrast, the kinetic traces for reduction of PSI from PsaA-W651F by cyt c_6 (Fig. 3*B*) as well as for reduction of PSI from PsaA-W651S (Fig. 3, *C* and *D*) by both donor molecules show a small contribution of a fast (μs) kinetic phase.

In further investigations of the kinetic components, the concentration of the donors was varied up to 300 μM for cyt c_6 and 200 μM for pc. The reaction rate k for the slower phase increased linearly with increasing concentrations for both donors and exhibited a slight saturation profile at high concentrations (Fig. 4). The second order rate constants k_2 were estimated to be 1.9×10^7 s^{-1} M^{-1} and 5.5×10^6 s^{-1} M^{-1} for the reduction of PSI from PsaA-W651F by pc and cyt c_6, respectively. These rates are 4- and 6-fold slower for pc and cyt c_6, respectively, than the rates obtained with wild-type PSI. For PSI from PsaA-W651S, second order rate constants of 3.1×10^7 s^{-1} M^{-1} and 2.1×10^6 s^{-1} M^{-1} for pc and cyt c_6, respectively (Fig. 4), were estimated, corresponding to a 3- and 16-fold decrease as compared with the rate for wild-type PSI.

Fig. 5 shows the relative amplitude of the fast phase A(1) of $P700^+$ reduction for the mutated PSI complexes in the presence of varying concentrations of soluble donors as indicated.

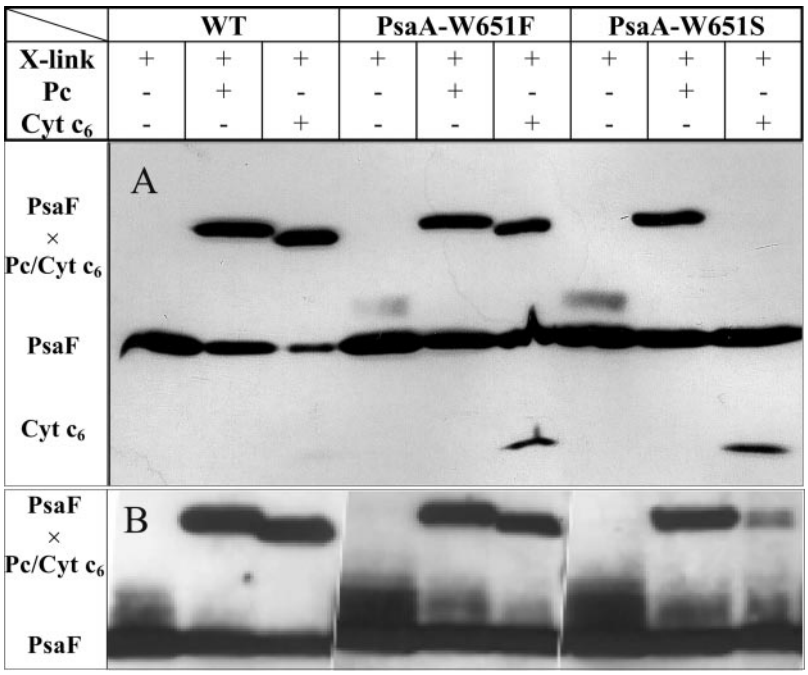

FIG. 2. **Cross-link of mutant photosystem PsaA-W651S with the electron donor cyt c_6 is strongly impaired.** *A* and *B* show independent experiments. The cross-linking reaction mixture (*X-link*) of pc or cyt c_6 and PSI (according to 2 μg of *Chlorophll*) from WT and mutants PsaA-W651F and PsaA-W651S was separated by SDS-PAGE and immuno-probed with anti-PsaF antibodies. The heme group of cyt c_6 is also detectable under these conditions (*A* and *B*). The exposure time of the immuno-detection in *experiment B* was prolonged to demonstrate cross-linking between cyt c_6 and PSI from mutant PsaA W651S.

The amplitude of the fast phase increased with increasing concentrations of cyt c_6 at the expense of the amplitude for the slower component A(2). The half-time of $t_{1/2}(1)$ of ~30 μs remained constant. For pc as a donor, no fast component could be observed with PSI from mutant PsaA-W651F at concentrations of pc up to 200 μM. However, with PSI containing the serine mutation PsaA-W651S, a fast kinetic component was visible, indicating that both donors were able to form a transient complex with this mutant of PSI. These data are similar to the results with PSI from mutant PsaB-W627F, where the first order electron transfer ($t_{1/2}(1)$) from cyt c_6 to P700 was slowed down by about a factor of 10 as compared with WT, whereas no first order component was detectable for pc as a donor (14).

Equation 1 indicates that the relative amplitude A(1) has a hyperbolic dependence of the donor concentration [D], *i.e.* shows a half-maximum saturation at a donor protein concentration equal to K_D and approaching a maximum value f at infinite concentration. For the binding of pc or cyt c_6 to wild-type PSI, the results were very close to the K_D values of 83 and 81 μM and f values of 0.67 and 0.68, respectively, found in the previous study (13). For PSI isolated from the PsaA mutant strains, from the data shown in Fig. 5, the maximum value of the amplitude A(1) at very high donor concentrations could only be estimated because the relative contribution of this kinetic component remained below 25% within the range of donor concentration exploited. The data are consistent with f values close to those found for the wild-type PSI, but it cannot be excluded that these maximum values are somewhat smaller in the mutants. Assuming values of f equal to the wild-type values, dissociation constants of about 1087 and 2560 μM for the binding of cyt c_6 to PSI from PsaA-W651F and PsaA-W651S, respectively, and about 554 μM for the binding of pc to PSI from PsaA-W651S have been determined from a curve fitting of Equation 1 (Fig. 5, *solid lines*) to the data points in Fig. 5. The dissociation constants for the two donors and the altered PSI, which are summarized in Table II, are considered as upper limits only. These values giving a measure of the binding affinity within the donor concentration range shown in Fig. 5 will be used to explore the effect of mutations on the binding behavior of the two donors.

Salt Dependence—Long range electrostatic interactions between the positively charged residues of PsaF and conserved acidic patches of pc or cyt c_6 play an important role in recognition and correct binding between the donor molecules and PSI, enabling fast and efficient electron transfer. Therefore, the salt dependence of the second order electron transfer rate constants for electron transfer between PSI and pc or cyt c_6 was investigated (Fig. 6). As described before, the second order rate constant decreases at increasing ionic strength for wild type and both donors (12–14). The same behavior was found at increasing salt concentrations for the electron transfer reaction between PSI from the PsaA mutant strains and the two donors.

Redox Potentiometry—The change of residues close to the special chlorophyll pair P700 could alter the $P700/P700^+$ redox midpoint potential. A change in the $P700/P700^+$ redox midpoint potential would in turn change the free energy of the electron transfer reaction. To test whether this is the case, we measured the $P700/P700^+$ redox midpoint potentials of PSI from the altered PsaA strains as well as from the strain PsaB-W627F. As shown in Table II, the redox midpoint potentials decreased only by 10 mV for the changes of Trp to Phe and remained constant for the change W651S as compared with WT. The standard deviations derived from the Nernst fits were approximately ±6.5 mV (including the calibration error). A change of 10 mV would slow down the half-life of the first order electron transfer reaction by about 0.5 μs using an approximation for electron transfer from Ref. 29 and a reorganization energy λ of 545 mV as estimated by Ramesh *et al.* (30). Even a decrease in driving force by 30 mV would only change the half-life of the first order electron transfer by 2.5 μs. Assuming that the reorganization energy λ remains unchanged, the difference in the redox midpoint potential cannot account for the observed differences in the first order electron transfer rates obtained for the donors and PSI from PsaA or the PsaB mutant strains. Our data would rather indicate that an alteration of the hydrophobic binding site induces a change in distance between the redox centers of the donors and P700, which is supposed to be in the range of 0.5–1 Å according to the estimations mentioned above.

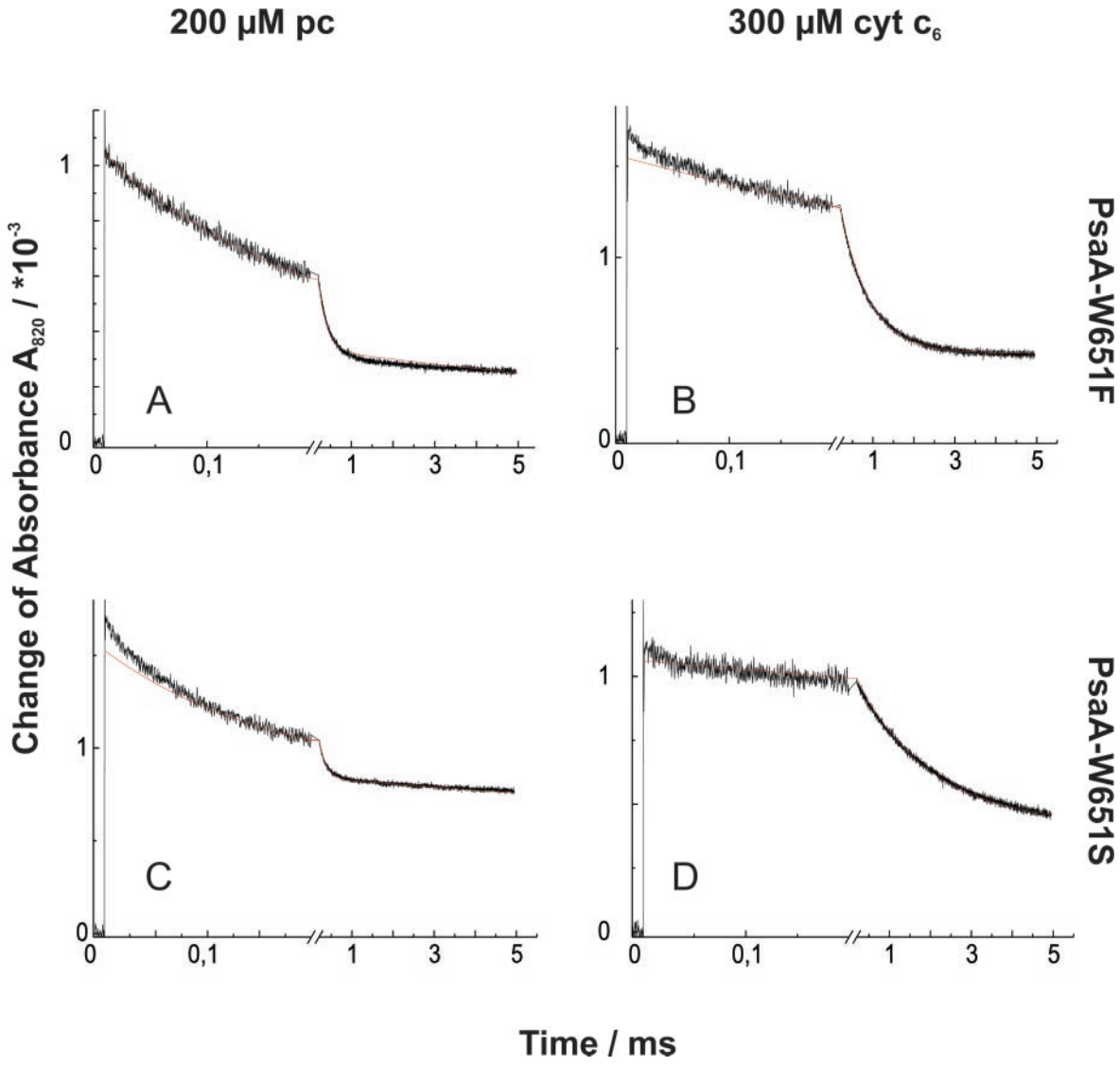

FIG. 3. **Kinetic traces for reduction of PSI PsaA-W651F (*A* and *B*) and PsaA-W651S (*C* and *D*) in the presence of 200 µM pc or 300 µM cyt c_6, respectively.** The *drawn curves* represent the absorption decays accounting only for the fitted slower second order phases. Only PSI PsaA-W651F/pc (*A*) shows a monoexponential decay, whereas the other traces, *B*–*D*, exhibit a fast first order phase with a half-life of about 15–30 µs.

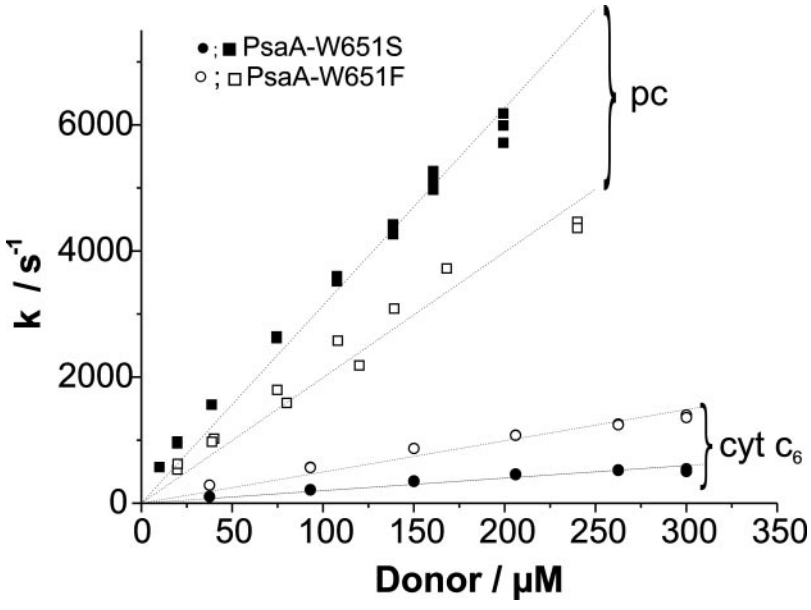

FIG. 4. **Determination of the second order rate constants for electron transfer between the two electron donors pc or cyt c_6 and PSI from PsaA-W651S (■; ●) or PsaA-W651F (□; ○).** The measurements were performed at optimal $MgCl_2$ concentration. For estimation of k_2, only measurements in the linear part were taken into account. Results are summarized in Table II.

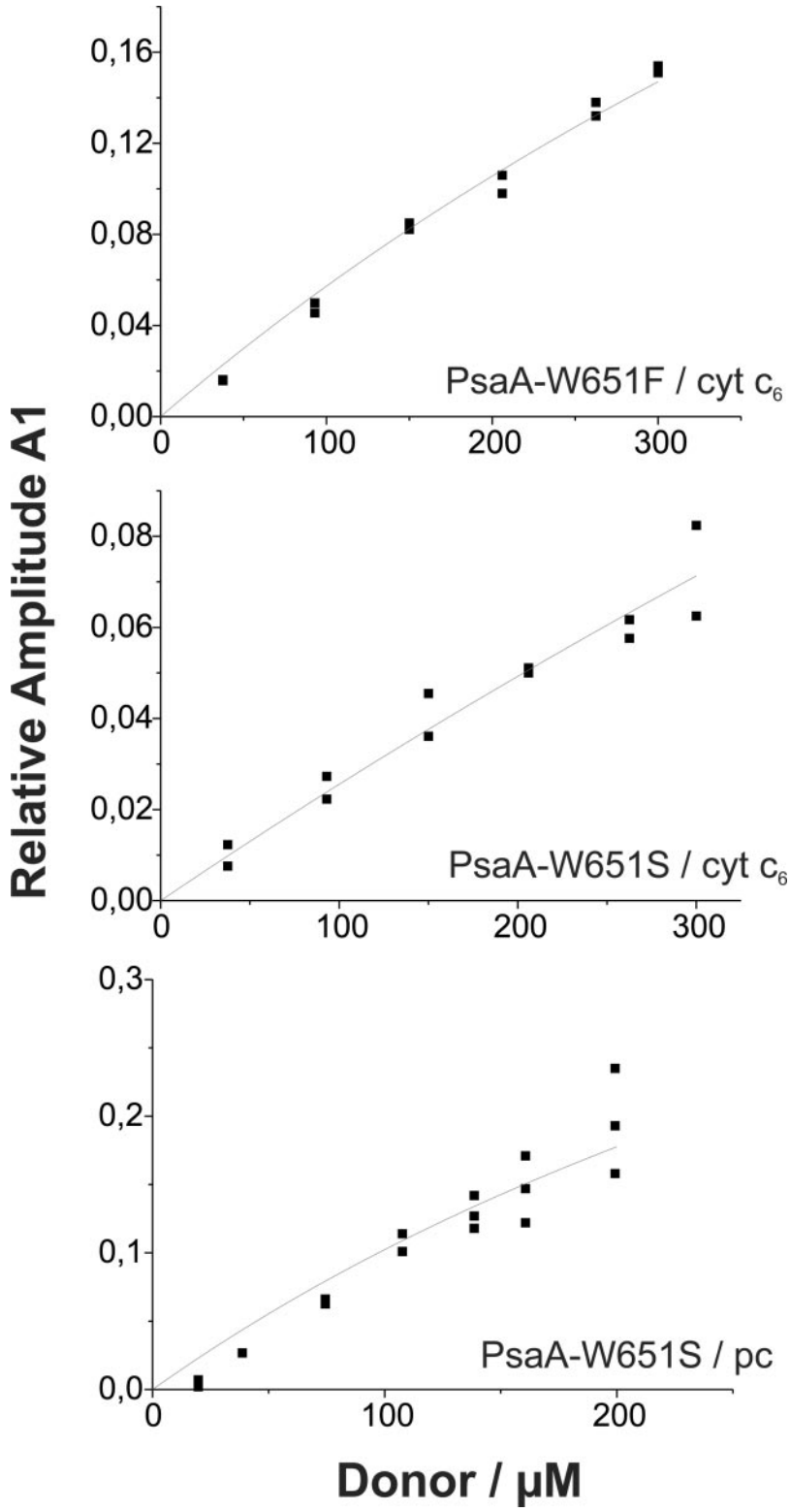

FIG. 5. **Relative amplitude of the fast kinetic phase of $P700^+$ reduction as a function of the donor concentration.** Determination of the dissociation constants for the electron transfer between the two donors and PSI with the altered PsaA was performed on two sets of data with each 10 averaged measurements. The *lines* represent fits with *f* values determined from the reaction with WT PSI of $f = 0.68$ or 0.67 for cyt c_6 or pc, respectively, and are in good approximation within the error of the experiments. Results are summarized in Table II.

DISCUSSION

In a previous study, we could show that residue PsaB-W627F is important for proper binding and efficient electron transfer from both pc and cyt c_6 to PSI (14). In this study, we have taken advantage of a PsaA-deficient mutant (24) to modify the PsaA-Trp^{651} using chloroplast transformation and site-directed mutagenesis. PSI particles from the mutant strains containing a specific amino acid change in the PsaA protein, W651F and W651S, were isolated together with PSI particles from wild type and used with purified pc and cyt c_6 to characterize the electron transfer between these donors and PSI *in vitro*. Our results indicate that PsaA-Trp^{651} together with PsaB-Trp^{627} forms the hydrophobic recognition site that is essential for binding of pc and cyt c_6 to the core of PSI. Our results also indicate that pc and cyt c_6 bind slightly different to the core of PSI since both donors are affected differently in their binding affinities by mutations at the positions of the two tryptophan amino acid residues.

As shown by Ref. 14, the mutation of PsaB-Trp^{627} to Phe abolished the formation of a stable first order electron transfer

TABLE II

P700 midpoint potentials and electron transfer properties from pc or cyt c_6 to PSI isolated from WT and the different strains mutated either on PsaA-Trp^{651} or PsaB-Trp^{627}

	Plastocyanin		Cytochrome c_6		Midpoint-potential
	k_2	K_D (*f*)	k_2	K_D (*f*)	E_m
	$s^{-1} \times 10^6$	μM	$s^{-1} \times 10^6$	μM	[*mV*] [b]
WT[a]	90	83 (f = 0.67)	34	81 (f = 0.68)	473
PsaA-W651F	19		5.5	1087 (f = 0.68)	463
PsaA-W651S	31	554 (f = 0.67)	2.1	2560 (f = 0.68)	477
PsaB-W627F [c]	6.4		16	177 (f = 0.66)	463

[a] Values for the kinetic constants were taken from Ref. 13.
[b] Standard deviations are ± 6.5 mV (from the Nernst fits and calibration).
[c] Values for the kinetic constants were taken from Ref. 14.

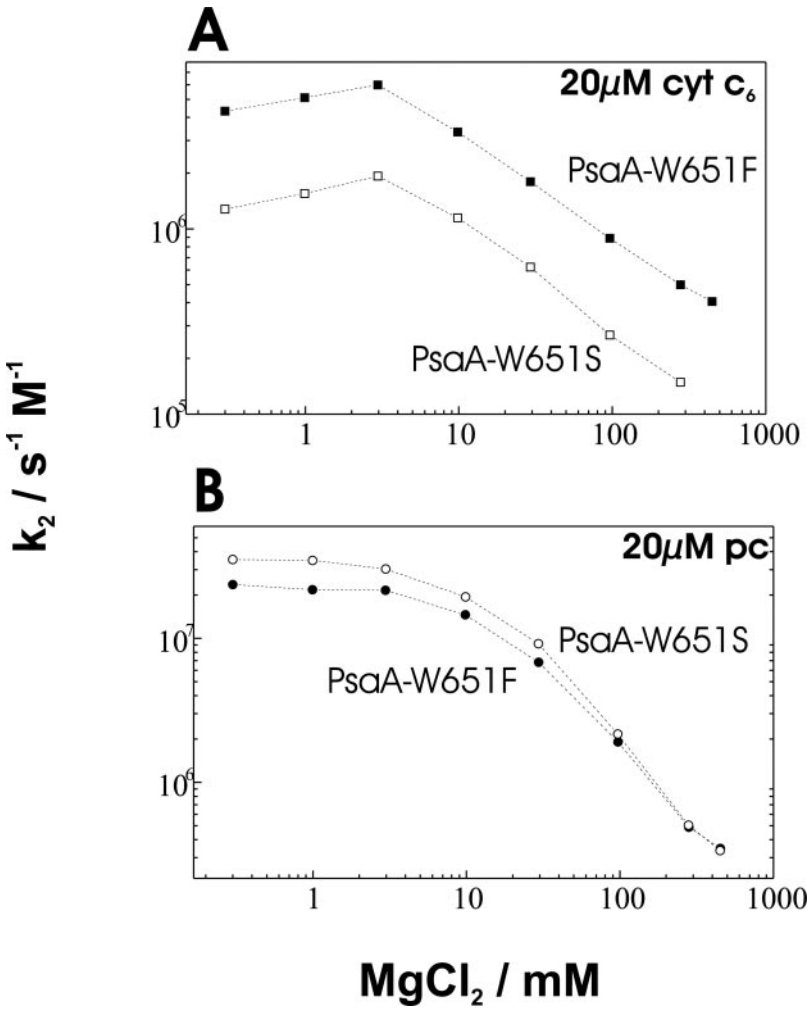

FIG. 6. **Dependence of the second order rate constant k_2 from the ionic strength.** Measurements were performed in the presence of 20 μM of the respective donor, and ionic strength was adjusted by adding small amounts of a concentrated $MgCl_2$ solution.

complex between pc and the altered PSI but allowed the formation of an inter-molecular electron transfer complex between cyt c_6 and the PsaB-W627F PSI. The corresponding mutation of PsaA-Trp^{651} to Phe had a similar impact. However, the dissociation constant for binding of cyt c_6 to PSI from PsaA-W651F was 3–5-fold larger than for the binding to PsaB-W627F PSI (Table II). In the same line, the rate constant for electron transfer between cyt c_6 and PSI from PsaA-W651F was about three times slower than for the electron transfer with PSI from PsaB-W627F. Mutation of PsaA-Trp^{651} to Ser had an even larger impact on the dissociation and rate constants. The K_D value increased, and the rate constant decreased another 2-fold when the values obtained for the interaction and electron transfer between cyt c_6 and PSI from PsaA-W651S and PsaA-W651F are compared (Table II). In contrast, binding and electron transfer of pc to PSI from PsaA-W651S improved as compared with PSI from PsaA-W651F. It is of note that rate constants for the electron transfer between pc and PSI from PsaA-W651F and PsaA-W651S increase 3- and 5-fold, respectively, as compared with the rate constant measured for PSI from PsaB-W627F. This indicates that alterations of PsaB-Trp^{627} or PsaA-Trp^{651} have different impacts on binding and electron transfer between the PsaA or PsaB mutant PSI and pc or cyt c_6. From these results, we can deduce that pc binds more tightly to the PsaB-Trp^{627}, whereas cyt c_6 interacts more directly with PsaA-Trp^{651}. This conclusion is also supported by the cross-linking experiments (Fig. 2), where the mutation PsaA-W651S almost completely abolished the formation of a cross-link product between PsaF and cyt c_6. In this case, the salt dependence of the second order rate constant k_2 suggested that the negatively charged cyt c_6 sensed the presence of the positively charged N-terminal domain of PsaF, which supports

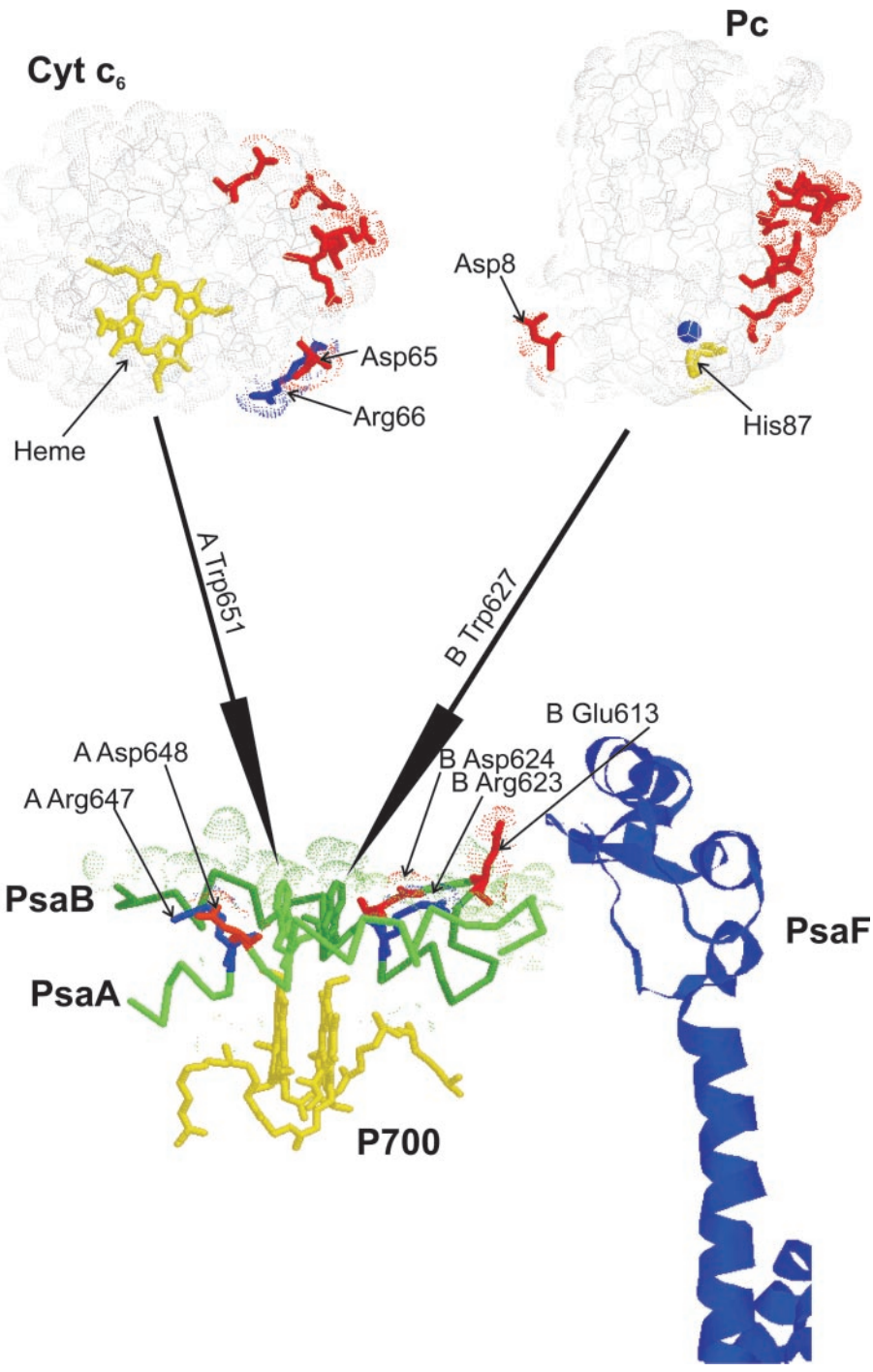

FIG. 7. **Crystal structures of *C. reinhardtii* cyt c_6 at a resolution of 1.6 Å (31) and of pc at 1.5 Å (35) as well as *S. elongatus* PSI at 2.5 Å (5) in a view along the membrane plane.** The numbering for all residues corresponds to the positions in *C. reinhardtii*. Positively charged residues as well as the copper center of pc are in *blue*, negatively charged residues in *red*, the residues involved in electron transfer of P700 and the heme group of cyt c_6 and His^{87} of pc are in *yellow*, and the two lumenal helices *l* and *l′* of PsaB and PsaA are in *darker* and *lighter green*, respectively. The PsaF subunit in eukaryotic PSI contains an N-terminal extension on the lumenal side of PSI presenting patches of positively charged residues that have been shown to interact with the negatively charged patches on the both donors and is orientated through close electrostatic interactions with PsaB-Glu^{613} (14).

our argumentation that residue PsaA-Trp^{651} is crucial for a productive formation of an electron transfer complex between PSI and cyt c_6.

Interestingly, the change of residue PsaA-Trp^{651} to the hydrophilic Ser restored slightly the formation of the electron transfer complex between pc and the altered PSI as compared with the interaction of pc with PSI from PsaA-W651F. It is tempting to speculate that a hydrophilic interaction between the Ser residue at position W651S and an appropriate residue on the surface of pc, eventually H87 on the "northern" hydrophobic interaction site of pc, results in an equivalent gain of binding energy that compensates the loss of hydrophobic interaction surface.

From a structural point of view (Fig. 7), other highly conserved residues on PsaA and PsaB that are exposed into the lumenal space could play a role in the interaction between pc or cyt c_6 and PSI, namely PsaA-Asp^{648} and Arg^{647} as well as PsaB-Asp^{624} and Arg^{623}. These charged compensated pairs enframe PsaA-Trp^{651} and PsaB-Trp^{627}. An equivalent pair is located at the northern face of cyt c_6 from *C. reinhardtii* (Asp^{65} and Arg^{66} (31)). Site-directed mutagenesis of pc or cyt c_6 from *Synechocystis* sp. PCC 6803 and *Anabaena* PCC 7119 and analysis of binding and electron transfer between the altered donors and the cyanobacterial PSI revealed that the positively charged amino acid located at the northern face of either pc or cyt c_6 is crucial for the interaction with the reaction center (32–34). Interestingly, an equivalent positively charged exposed amino acid is absent from pc of *C. reinhardtii* (Fig. 7) and other eukaryotic pc structures. By comparing the geometry and the distances as obtained from the structural data, electrostatic

interaction between Arg^{66}/Asp^{65} of cyt c_6 with Asp^{624}/Arg^{623} on PsaB appears to be feasible. On the other hand, an interaction of pc Asp^{8} with Arg^{647} on PsaA might be possible. Interestingly, geometry and distances are very similar for the conserved triplets PsaA-Trp^{651}/B-Asp^{624}/PsaB-Arg^{623} or PsaB-Trp^{627}/PsaA-Asp^{648}/A-Arg^{647}. In the case of prokaryotic PSI and prokaryotic donors, where the orientation for binding of the donors to the PSI is not restricted by correct interaction with the PsaF subunit, two symmetric orientations for the donor binding would be possible, favoring either of the two triplets. In such a way, the shape of the binding pocket would have changed from a symmetric to an asymmetric interface. The loss of the positively charged residue at the northern face of eukaryotic pc is in line with this consideration. *C. reinhardtii* cyt c_6 would therefore represent the ancient donor, whereas *C. reinhardtii* pc, the donor that is optimized to interact with the eukaryotic oxidizing side of PSI, which is characterized by the presence of the positively charged N-terminal domain of PsaF.

Acknowledgments—We are very grateful to Dr. K. Redding for the kind gift of various plasmids and the Δ*psaA* mutant strain of *C. reinhardtii*. We also thank Dr. J. D. Rochaix for the kind gift of antibodies.

REFERENCES

1. Wood, P. M. (1978) *Eur. J. Biochem.* **87,** 9–19
2. Ho, K. K., and Krogmann, D. W. (1984) *Biochim. Biophys. Acta* **766,** 310–316
3. Merchant, S., and Bogorad, L. (1986) *Mol. Cell. Biol.* **6,** 462–469
4. Sandmann, G. (1986) *Arch. Microbiol.* **21,** 6366–6375
5. Jordan, P., Fromme, P., Witt, H. T., Klukas, O., Saenger, W., and Krauss, N. (2001) *Nature* **411,** 909–917
6. Hippler, M., Rimbault, B., and Takahashi, Y. (2002) *Protist* **153,** 197–220
7. Setif, P. (2001) *Biochim. Biophys. Acta* **1507,** 161–179
8. Hippler, M., Reichert, J., Sutter, M., Zak, E., Altschmied, L., Schröer, U., Herrmann, R. G., and Haehnel, W. (1996) *EMBO J.* **15,** 6374–6384
9. Drepper, F., Hippler, M., Nitschke, W., and Haehnel, W. (1996) *Biochemistry* **35,** 1282–1295
10. Nordling, M., Sigfridsson, K., Young, S., Lundberg, L. G., and Hansson, O. (1991) *FEBS Lett.* **291,** 327–330
11. Haehnel, W., Jansen, T., Gause, K., Klosgen, R. B., Stahl, B., Michl, D., Huvermann, B., Karas, M., and Herrmann, R. G. (1994) *EMBO J.* **13,** 1028–1038
12. Hippler, M., Drepper, F., Farah, J., and Rochaix, J. D. (1997) *Biochemistry* **36,** 6343–6349
13. Hippler, M., Drepper, F., Haehnel, W., and Rochaix, J. D. (1998) *Proc. Natl. Acad. Sci. U. S. A.* **95,** 7339–7344
14. Sommer, F., Drepper, F., and Hippler, M. (2002) *J. Biol. Chem.* **277,** 6573–6581
15. Farah, J., Rappaport, F., Choquet, Y., Joliot, P., and Rochaix, J. D. (1995) *EMBO J.* **14,** 4976–4984
16. Hippler, M., Drepper, F., Rochaix, J. D., and Muhlenhoff, U. (1999) *J. Biol. Chem.* **274,** 4180–4188
17. Haldrup, A., Simpson, D. J., and Scheller, H. V. (2000) *J. Biol. Chem.* **275,** 31211–31218
18. Ben-Shem, A., Frolow, F., and Nelson, N. (2003) *Nature* **426,** 630–635
19. Chitnis, P. R., Purvis, D., and Nelson, N. (1991) *J. Biol. Chem.* **266,** 20146–20151
20. Xu, Q., Yu, L., Chitnis, V. P., and Chitnis, P. R. (1994) *J. Biol. Chem.* **269,** 3205–3211
21. Sun, J., Xu, W., Hervas, M., Navarro, J. A., Rosa, M. A., and Chitnis, P. R. (1999) *J. Biol. Chem.* **274,** 19048–19054
22. Harris, E. H. (1989) *The Chlamydomonas sourcebook: A comprehensive Guide to Biology and Laboratory Use*, Academic Press, San Diego
23. Sambrook, J., Fritsch, E. F., and Maniatis, T. (1989) in *Molecular Cloning: A Laboratory Manual* (Nolan, C., ed) 2nd Ed., Cold Spring Harbor Laboratory Press, Cold Spring Harbor, NY
24. Redding, K., MacMillan, F., Leibl, W., Brettel, K., Hanley, J., Rutherford, A. W., Breton, J., and Rochaix, J. D. (1998) *EMBO J.* **17,** 50–60
25. Goldschmidt-Clermont, M. (1991) *Nucleic Acids Res.* **19,** 4083–4089
26. Porra, R. J., Thompson, W. A., and Kriedemann, P. E. (1989) *Biochim. Biophys. Acta* **975,** 384–394
27. Laemmli, U. K. (1970) *Nature* **227,** 680–685
28. Sommer, F., Hippler, M., Biehler, K., Fischer, N., and Rochaix, J. D. (2003) *Plant Cell Environ.* **26,** 1881–1892
29. Moser, C. C., Keske, J. M., Warncke, K., Farid, R. S., and Dutton, P. L. (1992) *Nature* **355,** 796–802
30. Ramesh, V. M., Guergova-Kuras, M., Joliot, P., and Webber, A. N. (2002) *Biochemistry* **41,** 14652–14658
31. Kerfeld, C. A., Anwar, H. P., Interrante, R., Merchant, S., and Yeates, T. O. (1995) *J. Mol. Biol.* **250,** 627–647
32. De la Cerda, B., Diaz-Quintana, A., Navarro, J. A., Hervas, M., and De la Rosa, M. A. (1999) *J. Biol. Chem.* **274,** 13292–13297
33. Molina-Heredia, F. P., Diaz-Quintana, A., Hervas, M., Navarro, J. A., and De La Rosa, M. A. (1999) *J. Biol. Chem.* **274,** 33565–33570
34. Molina-Heredia, F. P., Hervas, M., Navarro, J. A., and De la Rosa, M. A. (2001) *J. Biol. Chem.* **276,** 601–605
35. Redinbo, M. R., Yeates, T. O., and Merchant, S. (1994) *J. Bioenerg. Biomembr.* **26,** 49–66